Hydration induced bandgap shift at pyrite-water interface

Haiyang Xian, Runxiang Du, Jianxi Zhu, Meng Chen, Wei Tan, Runliang Zhu, Jingming Wei, and Hongping He

Citation: Appl. Phys. Lett. **113**, 123901 (2018); doi: 10.1063/1.5048542
View online: https://doi.org/10.1063/1.5048542
View Table of Contents: http://aip.scitation.org/toc/apl/113/12
Published by the American Institute of Physics

Hydration induced bandgap shift at pyrite-water interface

Haiyang Xian[1,2,3] Runxiang Du[1,2,3] Jianxi Zhu[1,3,a)] Meng Chen[1,3] Wei Tan[1,3] Runliang Zhu[1,3] Jingming Wei[1,2,3] and Hongping He[1,2,3,a)]
[1]*CAS Key Laboratory of Mineralogy and Metallogeny/Guangdong Provincial Key Laboratory of Mineral Physics and Materials, Guangzhou Institute of Geochemistry, Chinese Academy of Sciences (CAS), Guangzhou 510640, China*
[2]*University of Chinese Academy of Sciences, Beijing 100049, China*
[3]*Institutions of Earth Science, Chinese Academy of Sciences, Beijing 100029, China*

(Received 16 July 2018; accepted 31 August 2018; published online 18 September 2018)

The practical application of earth abundant pyrite (FeS_2) in photovoltaic devices is extremely limited by the low open-circuit voltage (OCV) (~200 mV) induced low efficiency (<3%). As such, finding out the causes for the low OCV and the corresponding solutions has been widely concerned. Here, we report the hydration induced bandgap shift at the pyrite-water interface, which has been ignored in previous efforts. The bandgap shift may be one of the reasons responsible for the low OCV. Using *ab initio* calculations, we found that, compared to the pure pyrite surface in vacuum, the bandgap of the pyrite-water interfacial system possesses blue and red shifts at the water coverage of more and less than the mono-layer, respectively. The bandgap shift of the interfacial system could be explained by the adsorption symmetry and charge transfer between water and the substrate. These results reveal that the interfacial water could change the electronic structure of the pyrite surface, suggesting that hydration could be a highly probable stratagem to tune the photovoltage properties of pyrite-based materials. *Published by AIP Publishing.*
https://doi.org/10.1063/1.5048542

Pyrite (FeS_2) is a promising semiconducting material for solar photovoltaics due to its low cost (ranked number one in a recent cost analysis),[1] excellent absorptivity (of the order of $10^5\,cm^{-1}$),[2] and suitable bandgap (~0.95 eV).[3] The low open-circuit voltage (OCV) (~200 mV) induced low efficiency of pyrite photoelectrochemical cells (<3%) has been identified as the main barrier for its practical application since the 1980s.[2] Hence, it is important to recognize what is responsible for the low OCV and thereby figure out solutions to improve it.

To this end, much effort has been devoted to investigating the electronic structure of intrinsic, defective, and substituted pyrite in the past few decades.[7–12] Preliminary proposals regarding the cause of the low OCV of pyrite were mainly focused on intrinsic surface states and the presence of marcasite.[1,2,4–6] Nonetheless, these proposals were vetoed by later reports.[7,8] Alternatively, Zhang *et al.*[9] claimed that the low OCV can be caused by surface stoichiometry while Cabán-Acevedo *et al.*[8] and Lazić *et al.*[10] attributed the causes to ionization of high-density deep donor defect states and low intensity conduction states in pyrite, respectively. In the literature, substitution is a main approach for increasing the bandgap of pyrite, which may enlarge the OCV. Hu *et al.*[11] and Xiao *et al.*[12] reported that alloying with oxygen and zinc can increase the bandgap of pyrite.

In the practical application of pyrite in photovoltaic devices, the interaction between pyrite and ambient molecules such as water, which has been ignored in previous efforts, is sadly unavoidable. It is not known, however, if certain ambient factors could be the cause of the low bandgap and thereby the low OCV. Here, we report the effect of water molecules on the bandgap of the pyrite-water interface, which not only could be one of the reasons for the low OCV but also may be a highly possible stratagem to enhance the low OCV.

At the density functional theory (DFT) level, all the calculations in this study were performed by the Vienna Ab initio Simulation Package (VASP)[13] with the pseudopotential of projector augmented wave (PAW).[14] The Perdew-Burke-Ernzerhof (PBE) functions,[15] which have been shown to give good results for H_2O hydrogen bonding[16] and pyrite system,[17] were used to describe the exchange-correlation interaction among electrons. The cutoff energy was set to 350 eV (Ref. 9) for a 10^{-5} convergence of the total energy. PBE + U with a U-J parameter of 1.6 eV (Ref. 18) was employed to amend the bandgap of the interfacial system. Constant temperature *ab initio* molecular dynamics (AIMD) was performed using matrix diagonalization schemes along with Nosé-Hoover chain thermostats embedded in VASP.[19]

Our calculations were first validated by examining the adsorption energy and work function of the pyrite {100}-water interface in the ground state. The relaxed adsorption configurations show that the adsorbed water molecules interact with the substrate through O directing to the substrate, which is consistent with previous studies.[20,21] We also examined the work function of the configurations. The results in Fig. 1(a) show that the work function decreases monotonically with the increasing water coverage, agreeing with the experimental ultraviolet photoelectron spectroscopy of the pyrite-water interface.[22] Therefore, the model and method we employed are enough accurate to describe the pyrite-water system.

We then estimated the bandgap of the interfacial systems generated by the adsorption configuration from the geometry optimization. An interesting result is that the

a)Electronic addresses: zhujx@gig.ac.cn and hehp@gig.ac.cn

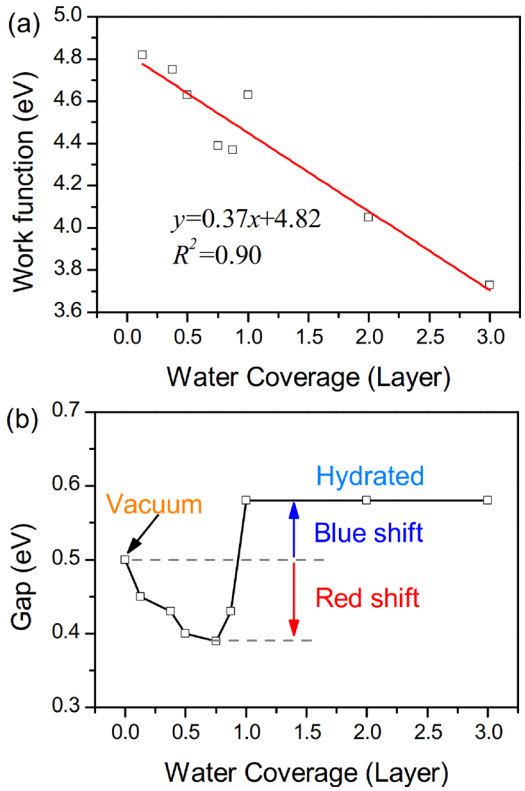

FIG. 1. (a) Work function and (b) bandgap of the pyrite-water interface as a function of water coverage in the ground state.

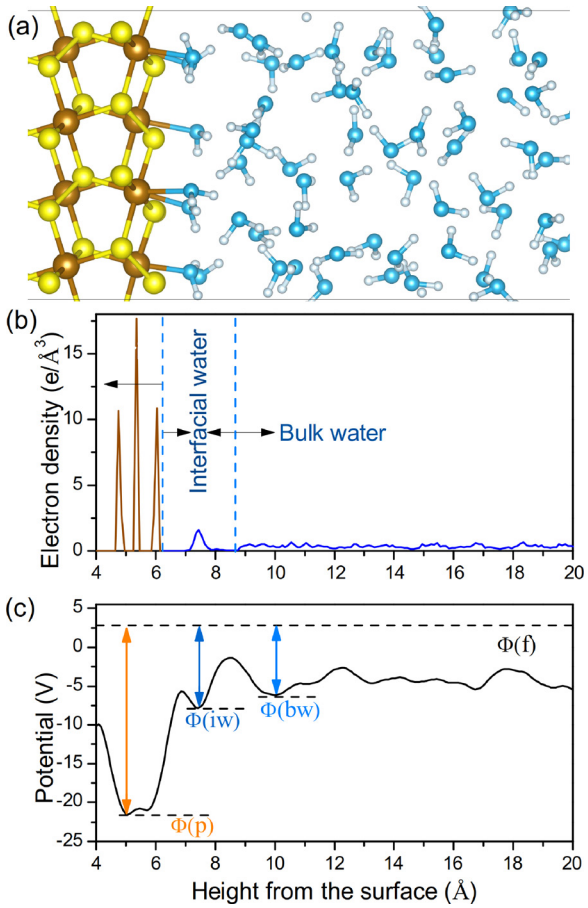

FIG. 2. Atomic structure and the corresponding atom density and local potential profile of the pyrite-water interface. (a) Structural schematic of the transition from the interfacial water ordered near pyrite surface (with an areal density of ~6.8 H_2O/nm^2) to bulk water (with a weight density of ~1.0 g/cm^3). (b) Planar average electron density along the c direction of the structural schematic. (c) Electrostatic potential profile of the interfacial system as a function of the distance above the pyrite surface. The variables Φ(p), Φ(iw), Φ(bw), and Φ(f) denote the position of pyrite, interfacial water, bulk water, and Fermi potentials for the interfacial system.

bandgap changes dramatically at different water coverages as shown in Fig. 1(b). The bandgap of the interfacial system shows red and blue shifts at the water coverage of less and more than one layer, respectively. The bandgap decreases first and then rises at the coverage of less than one layer. As the mono-water layer formed on the pyrite surface, the bandgap increases to larger than that of the pyrite surface in vacuum. As the water coverage increases to three layers, it still holds the same bandgap. The different gap shift of the interface at the water coverage of less than one layer may be caused by the symmetry change of the interfacial water at the *xy* plane because a similar gap shift by varying the symmetry is also found after adsorption of molecules on graphene.[23] The configurations with water coverage of less than one layer show lower symmetry than those with one-layer water coverage.

To clarify that if the bandgap shift displays the same trend at finite temperature, we performed an AIMD run with 104 waters filled into the vacuum, which gives a density of ~1.0 g/cm^3 aquatic environment. Like the adsorption mono-water layer structure, one distinct water layer at a height of ~1.5 Å above the pyrite surface sulfur could also be identified from the interfacial configuration of the AIMD run at 300 K as shown in Fig. 2(a). The mono-layer interfacial waters are stably absorbed on the pyrite surface with the oxygen interacting with the surface iron atoms during the AIMD run, consistent with the previous calculation.[20] Nevertheless, it is hard to directly recognize if there is any other ordered water layer beyond the monolayer from the configurations. Using an extended plug-in for VMD developed by Giorgino,[24] we calculated the electron density profile shown in Fig. 2(b) from the 1000 AIMD configurations to further characterize the interfacial water layer structure. The electron density profile shows one distinctive peak at a height of 1.46 Å above the outmost sulfur atoms, which corresponds to the first mono-layer water, and a horizontal line with small fluctuations, which arise from the stochastic volatility of the bulk-like water. The fluctuations may be caused by the limit of the AIMD time, 1 ps. We also employ the electrostatic potential of the pyrite-water interface, as shown in Fig. 2(c), to describe the water layer structure. It is easy to identify the potential positions of the pyrite Φ(p), interfacial water Φ(iw), and bulk water Φ(bw), which obviously validate only one distinct water layer at the pyrite-water interface.

We then calculated the bandgap of the hydrated system. The bandgap of the interfacial system was performed on the configurations during the AIMD run with the PBE level of DFT. As shown in Fig. 3(a), the average bandgap of the hydrated system is 0.68 ± 0.02 eV while that of the pyrite {100} surface in vacuum is 0.50 eV, indicating a 0.18 eV blue shift after hydration. Because the standard PBE method always underestimates the bandgap of semiconductors,[25] the PBE + *U* approach with a *U*-*J* parameter of 1.6 eV, which

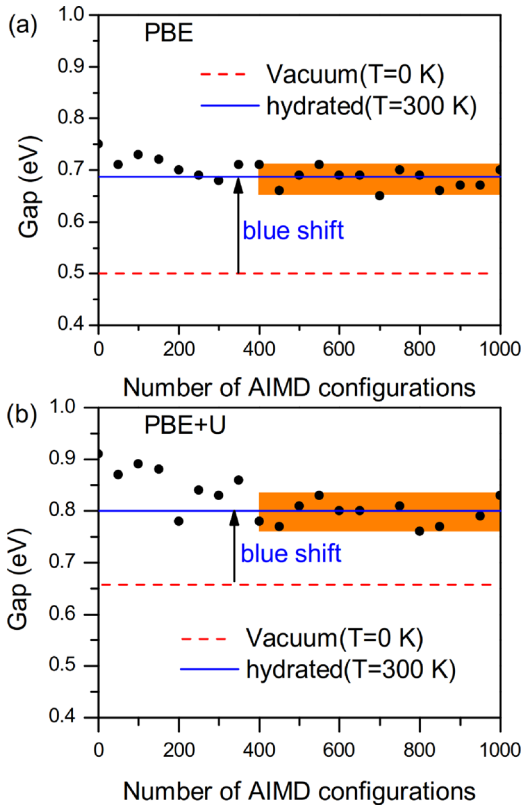

FIG. 3. Bandgaps during the *ab initio* molecular dynamics run of the hydrated pyrite {100} surface at 300 K using the (a) PBE and (b) PBE + U levels of DFT.

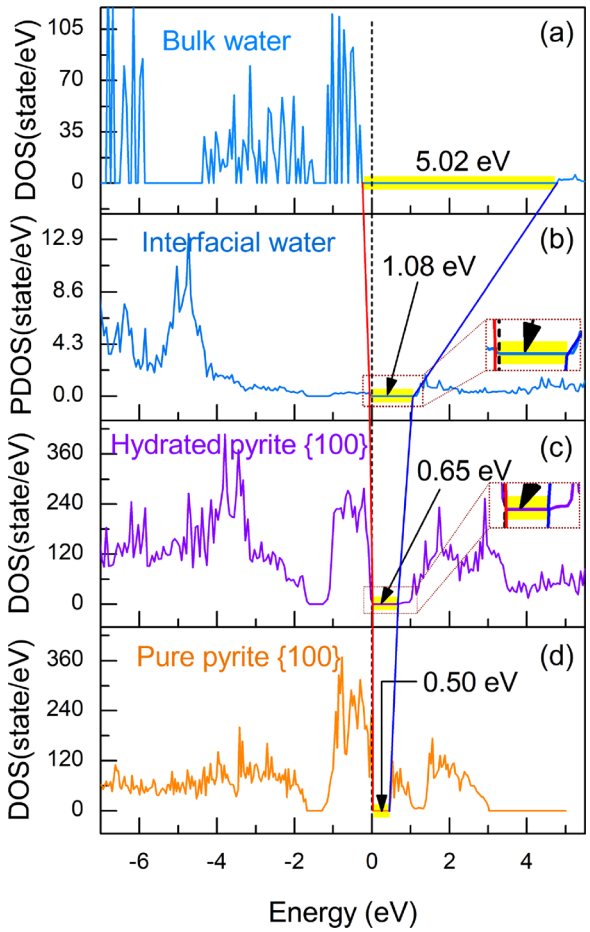

FIG. 4. (Partial) density of states (DOS/PDOS) of the pyrite-water interface from a randomly selected configuration during the AIMD run. (a) DOS of bulk water. (b) PDOS of the first layer interfacial water. (c) DOS of the hydrated pyrite {100} surface. (d) DOS of the pure pyrite {100} surface in vacuum.

gives good results consistent with the experimental bandgap,[18] was introduced to amend the deviation. The bandgaps from the PBE + U approach in Fig. 3(b) also show a 0.12 eV blue shift from 0.66 eV in vacuum (at 0 K) to 0.80 ± 0.02 eV in water (at 300 K). Although there is a little difference between the results from PBE and PBE + U, which may be caused by the methodical error, the hydrated system shows the same bandgap shift tendency as obtained from the calculations in the ground state.

To examine the causes of the opening of the bandgap after hydration, we compared the calculated density of states (DOS) of the hydrated system at finite temperature. On the one hand, the DOS of interfacial water as shown in Fig. 4(b) is totally different from that of bulk water as shown in Fig. 4(a). Both the main peaks of the valence band and the lowest conduction band of the interfacial water shift to lower energy. The shift of the DOS, then, changes the bandgap of water from 5.02 eV in the bulk to 1.08 eV at the interface, indicating that the properties of the interfacial water are largely different from that of the bulk water. This could be attributed to the dielectric constant altering of water at the solid-water interface.[26] On the other hand, the main conduction band peaks of the hydrated pyrite {100} surface as shown in Fig. 4(c) shift to higher energy than that of the pure pyrite {100} surface as shown in Fig. 4(d), which leads to a blue shift of the bandgap from 0.50 to 0.65 eV. Comparing the DOSs of interfacial water and the hydrated system, we found a strong interaction between the pyrite {100} surface and the bonded water layer at 1–3 and −1 to −4 eV in the conduction and valence bands, respectively.

The charge transfer (CT) may also be one reason for the DOS and bandgap shift. Using the Bader charge-division scheme,[27,28] we calculated the Bader charge of the pyrite-water interfacial system. We divided the atoms in the pyrite-water interfacial system into two types, the interfacial and bulk atoms. The bulk atoms include both bulk pyrite and bulk water molecules. The Bader charge results (Table S2 in the supplementary material) show that, compared to the bulk atoms, the charge of all the interfacial atoms changes distinctly except H, indicating that charge transfer occurs between interfacial Fe, S, and O at the interface. The Bader charges were used to estimate the charge transfer (CT) between pyrite and water. The results (Table S3 in the supplementary material) show distinct CT from interfacial water to pyrite, indicating that the pyrite surface is slightly reduced by the interfacial waters. Based on the Bader charge of the interfacial and bulk atoms (Table S2 in the supplementary material), we induce that the interfacial Fe was oxidized while the S was reduced by the interfacial water. Therefore, the CT from water to pyrite is a chief cause for the change in the electronic structure of interfacial water.

To summarize, we have demonstrated the bandgap shift at the pyrite-water interface, which not only could be the cause of the low OCV in photovoltaic devices but also provides potential to promote the OCV. The bandgap of the

interfacial system shows red and blue-shifts at the water coverage of less and more than one layer, respectively. The difference of the shift direction may be caused by the symmetry alteration of the adsorption configuration of the interfacial water layer. The gap shift is caused by the charge transfer from interfacial water to the pyrite surface, which induces slight reduction of sulfur and oxidation of iron on the pyrite surface. The results disclose the electronic properties of the pyrite-water interface as a function of water coverage, providing a framework to tune the bandgap of pyrite by hydration.

See supplementary material for details of computational details, adsorption energy, and charge transfer data from the interfacial water molecules to pyrite.

This work was supported by the National Natural Science Foundation of China (Grant No. 41573112) and the CAS/SAFEA International Partnership Program for Creative Research Teams (20140491534). This is contribution No. IS-2577 from GIGCAS.

[1]C. Wadia, A. P. Alivisatos, and D. M. Kammen, Environ. Sci. Technol. **43**, 2072 (2009).
[2]A. Ennaoui, S. Fiechter, C. Pettenkofer, N. Alonsovante, K. Buker, M. Bronold, C. Hopfner, and H. Tributsch, Sol. Energy Mater. Sol. Cells **29**, 289 (1993).
[3]D. Banjara, Y. Malozovsky, L. Franklin, and D. Bagayoko, AIP Adv. **8**, 025212 (2018).
[4]M. Bronold, Y. Tomm, and W. Jaegermann, Surf. Sci. **314**, L931 (1994).
[5]G. Z. Qiu, Q. Xiao, and Y. H. Hu, Comput. Mater. Sci. **29**, 89 (2004).
[6]D. Spagnoli, K. Refson, K. Wright, and J. D. Gale, Phys. Rev. B **81**, 094106 (2010).
[7]R. S. Sun, M. K. Y. Chan, and G. Ceder, Phys. Rev. B **83**, 235311 (2011).
[8]M. Cabán-Acevedo, N. S. Kaiser, C. R. English, D. Liang, B. J. Thompson, H. E. Chen, K. J. Czech, J. C. Wright, R. J. Hamers, and S. Jin, J. Am. Chem. Soc. **136**, 17163 (2014).
[9]Y. N. Zhang, J. Hu, M. Law, and R. Q. Wu, Phys. Rev. B **85**, 085314 (2012).
[10]P. Lazic, R. Armiento, F. W. Herbert, R. Chakraborty, R. Sun, M. K. Y. Chan, K. Hartman, T. Buonassisi, B. Yildiz, and G. Ceder, J. Phys.-Condens. Matter **25**, 465801 (2013).
[11]J. Hu, Y. N. Zhang, M. Law, and R. Q. Wu, J. Am. Chem. Soc. **134**, 13216 (2012).
[12]P. Xiao, X.-L. Fan, H. Zhang, X. Fang, and L.-M. Liu, J. Alloys Compd. **629**, 43 (2015).
[13]G. Kresse and J. Furthmuller, Comput. Mater. Sci. **6**, 15 (1996).
[14]G. Kresse and D. Joubert, Phys. Rev. B **59**, 1758 (1999).
[15]J. P. Perdew, K. Burke, and M. Ernzerhof, Phys. Rev. Lett. **77**, 3865 (1996).
[16]D. R. Hamann, Phys. Rev. B **55**, R10157 (1997).
[17]D. R. Alfonso, J. Phys. Chem. C **114**, 8971 (2010).
[18]A. Krishnamoorthy, F. W. Herbert, S. Yip, K. J. Van Vliet, and B. Yildiz, J. Phys.-Condens. Matter **25**, 045004 (2013).
[19]G. J. Martyna, M. L. Klein, and M. Tuckerman, J. Chem. Phys. **97**, 2635 (1992).
[20]A. Stirling, M. Bernasconi, and M. Parrinello, J. Chem. Phys. **119**, 4934 (2003).
[21]J. H. Chen, X. H. Long, and Y. Chen, J. Phys. Chem. C **118**, 11657 (2014).
[22]C. Pettenkofer, W. Jaegermann, and M. Bronold, Ber. Bunsen-Ges.-Phys. Chem. **95**, 560 (1991).
[23]J. Berashevich and T. Chakraborty, Phys. Rev. B **80**, 033404 (2009).
[24]T. Giorgino, Comput. Phys. Commun. **185**, 317 (2014).
[25]I. de, P. R. Moreira, F. Illas, and R. L. Martin, Phys. Rev. B **65**, 155102 (2002).
[26]O. Teschke, G. Ceotto, and E. F. De Souza, Chem. Phys. Lett. **326**, 328 (2000).
[27]R. F. Bader, *Atoms in Molecules* (Wiley Online Library, 1990).
[28]G. Henkelman, A. Arnaldsson, and H. Jonsson, Comput. Mater. Sci. **36**, 354 (2006).